

Small- x Asymptotics of the Quark Helicity Distribution: Analytic Results

Yuri V. Kovchegov^a, Daniel Pitonyak^b, Matthew D. Sievert^c

^a*Department of Physics, The Ohio State University, Columbus, OH 43210, USA*

^b*Division of Science, Penn State University-Berks, Reading, PA 19610, USA*

^c*Theoretical Division, Los Alamos National Laboratory, Los Alamos, NM 87545, USA*

Abstract

In this Letter, we analytically solve the evolution equations for the small- x asymptotic behavior of the (flavor singlet) quark helicity distribution in the large- N_c limit. These evolution equations form a set of coupled integro-differential equations, which previously could only be solved numerically. This approximate numerical solution, however, revealed simplifying properties of the small- x asymptotics, which we exploit here to obtain an analytic solution. We find that the small- x power-law tail of the quark helicity distribution scales as $\Delta q^S(x, Q^2) \sim (\frac{1}{x})^{\alpha_h}$ with $\alpha_h = \frac{4}{\sqrt{3}} \sqrt{\frac{\alpha_s N_c}{2\pi}}$, in excellent agreement with the numerical estimate $\alpha_h \approx 2.31 \sqrt{\frac{\alpha_s N_c}{2\pi}}$ obtained previously. We then verify this solution by cross-checking the predicted scaling behavior of the auxiliary “neighbor dipole amplitude” against the numerics, again finding excellent agreement.

Keywords:

PACS: 12.38.-t, 12.38.Bx, 12.38.Cy

1. Introduction

The small- x power-law behavior of parton distribution functions (PDFs) and hadronic structure functions at small Bjorken x is governed by quantum evolution equations which resum large logarithms of $\frac{1}{x}$. The most familiar of these is the linear Balitsky-Fadin-Kuraev-Lipatov (BFKL) equation [1, 2] for the unpolarized structure functions F_1 and F_2 along with the quark and gluon PDFs at small x , which resums the single-logarithmic parameter $\alpha_s \ln \frac{1}{x} \sim 1$ (with α_s the strong coupling constant). The result of this resummation is a power-law growth at small x given by $F_1(x, Q^2) \sim q(x, Q^2) \sim (\frac{1}{x})^{\alpha_p}$, with the leading-order (LO) exponent $\alpha_p = 1 + \frac{4\alpha_s N_c}{\pi} \ln 2$ known as the perturbative “Pomeron intercept” in the terminology of Regge theory. Here N_c is the number of colors.

The analogous small- x asymptotic behavior of the helicity PDFs $\Delta f(x, Q^2)$ and the polarized structure function $g_1(x, Q^2)$ has received much less attention than the unpolarized case. Early studies emphasized the role of exchanging polarized quarks [3–8] (the “Reggeon” in Regge theory), with important progress on the full polarized evolution made by Bartels, Ermolaev, and Ryskin [9, 10]. Recently, we have derived the small- x evolution equations for the quark helicity PDFs $\Delta q^S(x, Q^2)$ and the polarized structure function $g_1(x, Q^2)$ [11, 12] in the modern language of the dipole model. (In this Letter, we restrict

our discussion to the flavor-singlet quark helicity distribution; for the non-singlet quark helicity distribution, see [12].) These helicity evolution equations, like the perturbative Reggeon evolution equations, resum the double-logarithmic parameter $\alpha_s \ln^2 \frac{1}{x} \sim 1$; they couple to both polarized quark and gluon exchange, and, in this respect, differ from the gluon-only unpolarized LO BFKL equation.

In general, the helicity evolution equations derived in [11, 12] form an infinite tower of operator equations analogous to the Balitsky hierarchy [13, 14] for the unpolarized small- x evolution [14–21]. In both cases, the operator hierarchy closes in the large- N_c limit [14–17]. For helicity evolution, this still yields a pair of coupled integro-differential equations for the “polarized dipole amplitude” $G(x_{10}^2, z)$ and the auxiliary “neighbor dipole amplitude” $\Gamma(x_{10}^2, x_{21}^2, z)$ that must be solved to determine the power-law behavior at small x . (Here x_{ij} ’s denote transverse sizes of dipoles and z is the softest longitudinal momentum fraction between the quark and antiquark in the dipole.) This asymptotic behavior of the polarized dipole $G(x_{10}^2, z) \sim (zs)^{\alpha_h}$ determines the corresponding small- x asymptotics of the helicity PDFs and the polarized structure function: $\Delta q^S(x, Q^2) \sim g_1(x, Q^2) \sim (\frac{1}{x})^{\alpha_h}$, where we refer to the exponent α_h as the “helicity intercept” in analogy to the Pomeron intercept.

In [22], we solved the large- N_c helicity evolution equations for α_h numerically, obtaining $\alpha_h \approx 2.31 \sqrt{\frac{\alpha_s N_c}{2\pi}}$. We also found that such an intercept could lead to a significant enhancement of the contribution from the quark spin $\Delta\Sigma$ to the proton spin [22], which is not ruled out by cur-

Email addresses: kovchegov.1@osu.edu (Yuri V. Kovchegov), dap67@psu.edu (Daniel Pitonyak), sievertmd@lanl.gov (Matthew D. Sievert)

rent experimental data [23]. In the following Sections, we use an emergent scaling feature of this numerical solution, namely, that G depends only on a single combination of its arguments and not on each independently, to derive an analytic expression for α_h .

2. Solution of the large- N_c equations

In standard coordinates, the large- N_c helicity evolution equations read [11, 12]

$$G(x_{10}^2, z) = G^{(0)}(x_{10}^2, z) + \frac{\alpha_s N_c}{2\pi} \int_{\frac{1}{x_{10}^2 s}}^z \frac{dz'}{z'} \int_{\frac{1}{z' s}}^{x_{10}^2} \frac{dx_{21}^2}{x_{21}^2} \times \left[\Gamma(x_{10}^2, x_{21}^2, z') + 3G(x_{21}^2, z') \right], \quad (1a)$$

$$\Gamma(x_{10}^2, x_{21}^2, z') = G^{(0)}(x_{10}^2, z') + \frac{\alpha_s N_c}{2\pi} \int_{\frac{1}{x_{10}^2 s}}^{z'} \frac{dz''}{z''} \times \int_{\frac{1}{z'' s}}^{\min\left\{x_{10}^2, x_{21}^2 \frac{z'}{z''}\right\}} \frac{dx_{32}^2}{x_{32}^2} \left[\Gamma(x_{10}^2, x_{32}^2, z'') + 3G(x_{32}^2, z'') \right], \quad (1b)$$

where x_{10}, x_{21}, x_{32} are the transverse sizes of various dipoles and z, z', z'' are longitudinal momentum fractions of the softest (anti-)quarks in the dipoles. Following [22], it is convenient to introduce the scaled logarithmic variables

$$\eta \equiv \sqrt{\frac{\alpha_s N_c}{2\pi}} \ln \frac{zs}{\Lambda^2}, \quad s_{10} \equiv \sqrt{\frac{\alpha_s N_c}{2\pi}} \ln \frac{1}{x_{10}^2 \Lambda^2}, \quad (2a)$$

$$\eta' \equiv \sqrt{\frac{\alpha_s N_c}{2\pi}} \ln \frac{z's}{\Lambda^2}, \quad s_{21} \equiv \sqrt{\frac{\alpha_s N_c}{2\pi}} \ln \frac{1}{x_{21}^2 \Lambda^2}, \quad (2b)$$

$$\eta'' \equiv \sqrt{\frac{\alpha_s N_c}{2\pi}} \ln \frac{z''s}{\Lambda^2}, \quad s_{32} \equiv \sqrt{\frac{\alpha_s N_c}{2\pi}} \ln \frac{1}{x_{32}^2 \Lambda^2}, \quad (2c)$$

where Λ is an IR momentum cutoff and s is the center-of-mass-energy squared at which the helicity PDF is measured. In terms of these rescaled variables, the large- N_c helicity evolution equations are

$$G(s_{10}, \eta) = G^{(0)}(s_{10}, \eta) + \int_{s_{10}}^{\eta} d\eta' \int_{s_{10}}^{\eta'} ds_{21} \left[\Gamma(s_{10}, s_{21}, \eta') + 3G(s_{21}, \eta') \right], \quad (3a)$$

$$\Gamma(s_{10}, s_{21}, \eta') = G^{(0)}(s_{10}, \eta') + \int_{s_{10}}^{\eta'} d\eta'' \int_{\max\{s_{10}, s_{21} + \eta'' - \eta'\}}^{\eta''} ds_{32} \times \left[\Gamma(s_{10}, s_{32}, \eta'') + 3G(s_{32}, \eta'') \right]. \quad (3b)$$

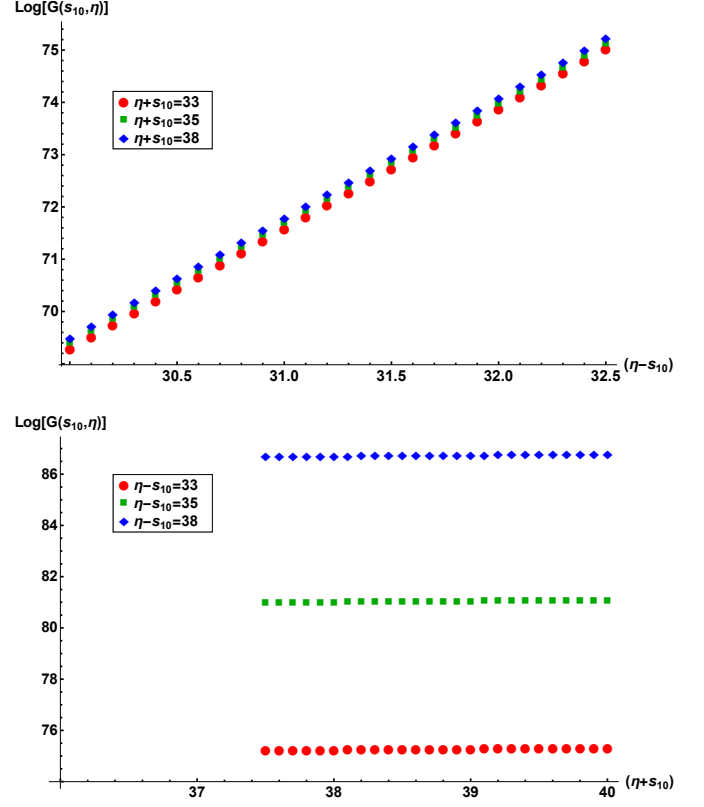


Figure 1: Numerical solution of the scaled equations (3) as a function of $\eta - s_{10}$ for fixed $\eta + s_{10}$ (top panel) and as a function of $\eta + s_{10}$ for fixed $\eta - s_{10}$ (bottom panel). The grid parameters are $\eta_{max} = 40, \Delta\eta = 0.05$. One clearly sees that $\ln G$ has a linear dependence on $\eta - s_{10}$ and is independent of $\eta + s_{10}$.

In the numerical solution of [22], two important features were observed in the asymptotic limit: (a) a negligible dependence on the choice of initial conditions $G^{(0)}$ and (b) the dependence of G only on the combination $\zeta \equiv \eta - s_{10}$, rather than on η and s_{10} separately (see Fig. 1). Let us therefore (a) trivially fix the initial conditions to $G^{(0)} = 1$ and (b) assume the $\eta - s_{10}$ scaling from the outset:

$$G(s_{10}, \eta) = G(\eta - s_{10}), \quad (4a)$$

$$\Gamma(s_{10}, s_{21}, \eta') = \Gamma(\eta' - s_{10}, \eta' - s_{21}). \quad (4b)$$

Then Eqs. (3) become

$$G(\zeta) = 1 + \int_0^{\zeta} d\xi \int_0^{\xi} d\xi' \left[\Gamma(\xi, \xi') + 3G(\xi') \right], \quad (5a)$$

$$\Gamma(\zeta, \zeta') = 1 + \int_0^{\zeta} d\xi \int_0^{\xi} d\xi' \left[\Gamma(\xi, \xi') + 3G(\xi') \right] + \int_{\zeta'}^{\zeta} d\xi \int_0^{\zeta'} d\xi' \left[\Gamma(\xi, \xi') + 3G(\xi') \right]$$

$$= G(\zeta') + \int_{\zeta'}^{\zeta} d\xi \int_0^{\xi'} d\xi' [\Gamma(\xi, \xi') + 3G(\xi')], \quad (5b)$$

with the boundary conditions

$$G(0) = 1, \quad \Gamma(\zeta', \zeta') = G(\zeta'). \quad (6)$$

Since $s_{10} \leq s_{21}$, we consider $\Gamma(\zeta, \zeta')$ only in the range $\zeta > \zeta'$.

To solve (5), we first differentiate, obtaining

$$\partial_{\zeta} G(\zeta) = \int_0^{\zeta} d\xi' [\Gamma(\zeta, \xi') + 3G(\xi')], \quad (7a)$$

$$\partial_{\zeta} \Gamma(\zeta, \zeta') = \int_0^{\zeta'} d\xi' [\Gamma(\zeta, \xi') + 3G(\xi')], \quad (7b)$$

and we then introduce the Laplace transforms

$$G(\zeta) = \int \frac{d\omega}{2\pi i} e^{\omega \zeta} G_{\omega}, \quad \Gamma(\zeta, \zeta') = \int \frac{d\omega}{2\pi i} e^{\omega \zeta'} \Gamma_{\omega}(\zeta), \quad (8a)$$

$$G_{\omega} = \int_0^{\infty} d\zeta e^{-\omega \zeta} G(\zeta), \quad \Gamma_{\omega}(\zeta) = \int_0^{\infty} d\zeta' e^{-\omega \zeta'} \Gamma(\zeta, \zeta'). \quad (8b)$$

Consider first the Laplace transform (8) of Eq. (7b),

$$\partial_{\zeta} \Gamma_{\omega}(\zeta) = \frac{1}{\omega} [\Gamma_{\omega}(\zeta) + 3G_{\omega}]. \quad (9)$$

This is just an ordinary differential equation in ζ , with the solution

$$\Gamma_{\omega}(\zeta) + 3G_{\omega} = e^{\frac{\zeta}{\omega}} [\Gamma_{\omega}(0) + 3G_{\omega}]; \quad (10)$$

substituting (10) back into (8) then gives

$$\Gamma(\zeta, \zeta') = \int \frac{d\omega}{2\pi i} e^{\omega \zeta'} \left\{ e^{\frac{\zeta}{\omega}} [\Gamma_{\omega}(0) + 3G_{\omega}] - 3G_{\omega} \right\}, \quad (11)$$

or, equivalently,

$$\Gamma(\zeta, \zeta') + 3G(\zeta') = \int \frac{d\omega}{2\pi i} e^{\omega \zeta' + \frac{\zeta}{\omega}} [\Gamma_{\omega}(0) + 3G_{\omega}]. \quad (12)$$

Using the second boundary condition in (6), Eq. (12) then fixes G , giving the general solution for G and Γ as

$$G(\zeta) = \frac{1}{4} \int \frac{d\omega}{2\pi i} e^{(\omega + \frac{1}{\omega})\zeta} H_{\omega}, \quad (13a)$$

$$\begin{aligned} \Gamma(\zeta, \zeta') &= \int \frac{d\omega}{2\pi i} e^{\omega \zeta' + \frac{\zeta}{\omega}} H_{\omega} \\ &\quad - \frac{3}{4} \int \frac{d\omega}{2\pi i} e^{(\omega + \frac{1}{\omega})\zeta'} H_{\omega}, \end{aligned} \quad (13b)$$

where we have introduced the unknown function H_{ω} as

$$H_{\omega} \equiv \Gamma_{\omega}(0) + 3G_{\omega}. \quad (14)$$

It is useful to observe that, upon substituting Eq. (11) back into Eq. (7b), the consistency of the solution requires that

$$\int \frac{d\omega}{2\pi i} e^{\frac{\zeta}{\omega}} \frac{1}{\omega} H_{\omega} = 0. \quad (15)$$

Indeed, the ω contour in the Bromwich integral (8) runs parallel to the imaginary axis and to the right of all the poles of the integrand. Because the extra factor of $1/\omega$ in the integrand of Eq. (15) provides sufficient convergence at infinity, we can close the contour in the right half-plane, getting zero and confirming Eq. (15).

Finally, we can impose a further constraint on our results in Eqs. (13) by requiring them to also satisfy Eq. (7a). Plugging Eqs. (13) into Eq. (7a) and employing (15) gives the constraint

$$\int \frac{d\omega}{2\pi i} e^{\omega \zeta + \frac{\zeta}{\omega}} \left(\omega - \frac{3}{\omega} \right) H_{\omega} = 0. \quad (16)$$

It is convenient to define f_{ω} such that

$$H_{\omega} = \left(\frac{\omega}{\omega^2 - 3} \right) f_{\omega} \quad (17)$$

and expand f_{ω} in a Laurent series:

$$f_{\omega} = \sum_{n=-\infty}^{\infty} c_n \omega^n. \quad (18)$$

After expanding both f_{ω} with (18) and $e^{\zeta/\omega}$ in their respective series, we pick up the enclosed residues at $\omega = 0$ and obtain the constraint

$$\begin{aligned} 0 &= \int \frac{d\omega}{2\pi i} e^{\omega \zeta + \frac{\zeta}{\omega}} f_{\omega} \\ &= \sum_{n=-\infty}^{-1} c_n I_{-n-1}(2\zeta) + \sum_{n=0}^{\infty} c_n I_{n+1}(2\zeta) \\ &= c_{-1} I_0(2\zeta) + \sum_{n=1}^{\infty} (c_{n-1} + c_{-n-1}) I_n(2\zeta). \end{aligned} \quad (19)$$

Thus, we obtain $c_{-1} = 0$ and $c_n = -c_{-n-2}$ for $n \geq 0$, such that

$$f_{\omega} = \sum_{n=0}^{\infty} c_n \left(\omega^n - \frac{1}{\omega^{n+2}} \right). \quad (20)$$

However, we know that f_{ω} cannot contain large positive powers of ω , or else it would affect convergence at infinity and violate the consistency condition (15). Substituting (17) into (15) gives

$$0 = \int \frac{d\omega}{2\pi i} e^{\frac{\zeta}{\omega}} \frac{1}{\omega^2 - 3} f_{\omega}. \quad (21)$$

Taking $\zeta = 0$ for simplicity and using (20), we have

$$0 = \sum_{n=0}^{\infty} c_n \int \frac{d\omega}{2\pi i} \frac{1}{\omega^2 - 3} \left(\omega^n - \frac{1}{\omega^{n+2}} \right)$$

$$= \sum_{n=1}^{\infty} c_n \int \frac{d\omega}{2\pi i} \frac{\omega^n}{\omega^2 - 3}, \quad (22)$$

where for all sufficiently convergent integrals, we have closed the contour in the right-half plane and obtained zero. Therefore, the consistency condition (15) implies that $c_n = 0$ for $n \geq 1$, such that

$$H_\omega = c_0 \frac{\omega^2 - 1}{\omega(\omega^2 - 3)}. \quad (23)$$

The function (23) fixes the solution of the helicity evolution equations, giving for G in Eq. (13a)

$$G(\zeta) = \frac{c_0}{4} \int \frac{d\omega}{2\pi i} e^{\omega\zeta + \frac{\zeta}{\omega}} \frac{\omega^2 - 1}{\omega(\omega^2 - 3)}. \quad (24)$$

Using the first boundary condition in (6) at $\zeta = 0$ fixes the coefficient to $c_0 = 4$, after closing the contour in the left half-plane and collecting the residues at $\omega = 0, \pm\sqrt{3}$. Therefore, the complete asymptotic solution of the large- N_c helicity evolution equations is given by

$$G(\zeta) = \int \frac{d\omega}{2\pi i} e^{\omega\zeta + \frac{\zeta}{\omega}} \frac{\omega^2 - 1}{\omega(\omega^2 - 3)}, \quad (25a)$$

$$\begin{aligned} \Gamma(\zeta, \zeta') &= 4 \int \frac{d\omega}{2\pi i} e^{\omega\zeta' + \frac{\zeta}{\omega}} \frac{\omega^2 - 1}{\omega(\omega^2 - 3)} \\ &\quad - 3 \int \frac{d\omega}{2\pi i} e^{\omega\zeta' + \frac{\zeta'}{\omega}} \frac{\omega^2 - 1}{\omega(\omega^2 - 3)}. \end{aligned} \quad (25b)$$

The high-energy/small- x asymptotics of Eq. (25a), corresponding to $\zeta \sim \zeta' \gg 1$, are given by the right-most pole of the integrand at $\omega = +\sqrt{3}$. Keeping the contribution to (25) from this pole only, we obtain the final result

$$G(\zeta) \approx \frac{1}{3} e^{\frac{4}{\sqrt{3}}\zeta} \quad (26a)$$

$$\begin{aligned} \Gamma(\zeta, \zeta') &\approx \frac{1}{3} e^{\frac{4}{\sqrt{3}}\zeta'} \left(4e^{\frac{\zeta - \zeta'}{\sqrt{3}}} - 3 \right) \\ &= G(\zeta') \left(4e^{\frac{\zeta - \zeta'}{\sqrt{3}}} - 3 \right). \end{aligned} \quad (26b)$$

The asymptotic form of $G \sim e^{\frac{4}{\sqrt{3}}\zeta} \sim (zs)^{\alpha_h}$ in (26a) gives the analytic expression for the helicity intercept

$$\alpha_h = \frac{4}{\sqrt{3}} \sqrt{\frac{\alpha_s N_c}{2\pi}} \approx 2.3094 \sqrt{\frac{\alpha_s N_c}{2\pi}}, \quad (27)$$

in complete agreement with the numerical solution $\alpha_h \approx 2.31 \sqrt{\frac{\alpha_s N_c}{2\pi}}$ of [22]!

Finally, we note that (26b) makes a useful prediction for the form of Γ which can be straightforwardly tested against the existing numerical solution of [22]. In the units (2) used in the numerics, our analytic solution predicts that the ratio of Γ to G should scale as

$$\ln \left[\frac{\Gamma(s_{10}, s_{21}, \eta)}{G(s_{21}, \eta)} + 3 \right] = \ln 4 + \frac{1}{\sqrt{3}}(s_{21} - s_{10}). \quad (28)$$

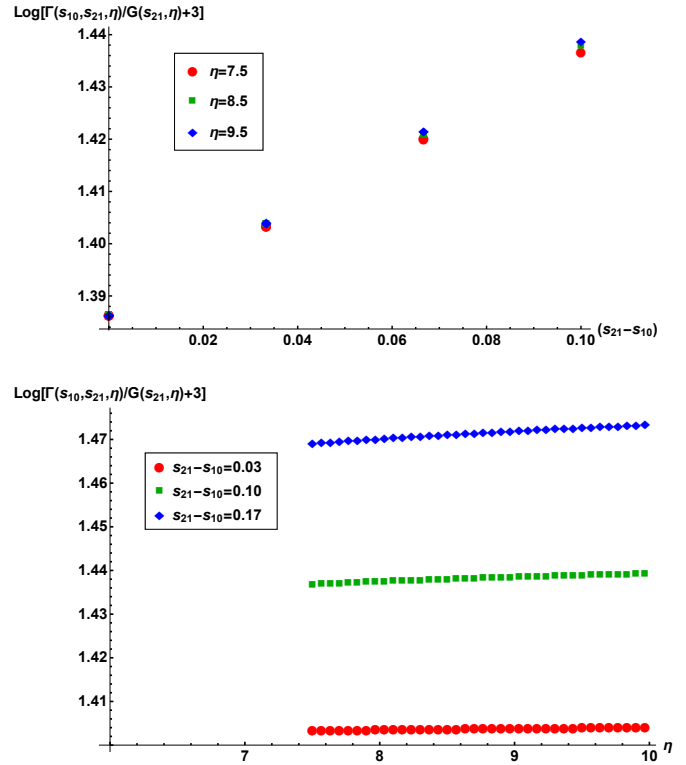


Figure 2: Plot of the scaling ratio (28) in the numerical solution of [22] as a function of $s_{21} - s_{10}$ for fixed η (top panel) and as a function of η for fixed $s_{21} - s_{10}$ (bottom panel). The grid parameters are $\eta_{max} = 10$, $\Delta\eta = 0.03$.

This ratio, calculated in the numerical solution of [22], is plotted in Fig. 2, where we see excellent agreement with the features of (28). Qualitatively, no dependence of this ratio on η is seen, and the dependence on $s_{21} - s_{10}$ is linear. And even though we have not performed a detailed extrapolation from the discretized numerics to the continuum, we even see significant quantitative agreement with (28): the vertical intercept (in the top panel of Fig. 2) of 1.386 agrees fantastically with the expected $\ln 4 \approx 1.3863$, and the slope of ≈ 0.52 is within 10% of the expected $\frac{1}{\sqrt{3}} \approx 0.577$. Indeed, if we perform a general fit of $\ln[\frac{\Gamma(s_{10}, s_{21}, \eta)}{G(s_{21}, \eta)} + 3]$ for $0 \leq s_{10} \leq s_{21} \leq 0.10$ and $7.5 \leq \eta \leq 10$ to a function of the form $as_{21} + bs_{10} + c\eta + d$, we find $a \approx -b \approx \frac{1}{\sqrt{3}}$ (within 10% accuracy) and $c \approx 0$, $d \approx \ln 4$ (with much greater accuracy). This preferred functional form is in excellent agreement with our analytic calculation (28). We also note that the numerics in [22] used scaling-violating initial conditions, so that the agreement seen here validates our claim of negligible dependence on the initial conditions. Thus, we can conclude with confidence that our analytic solution (26a) and helicity intercept (27) are the correct generalization of the numerical calculation in [22].

3. Conclusions

In this Letter, we have derived an analytic solution to the large- N_c helicity evolution equations (1) in the high-energy/small- x asymptotics. The central results are the solutions (26) for the polarized dipole amplitude G and the auxiliary neighbor dipole amplitude Γ , leading to the analytic expression for the helicity intercept (27). The key assumption which made such an analytic solution possible was the observation of emergent scaling behavior (4) as seen in the previous numerical solution of [22] (Fig. 1). We have checked our analytic results by comparing the predicted behavior of the auxiliary neighbor dipole amplitude Γ in Eq. (28) with the numerical solution in Fig. 2, finding excellent agreement.

Unfortunately, it is not clear whether the techniques used here can be extended to obtain an analytic solution of the helicity evolution equations in the large- N_c & N_f limit [11, 12]. The addition of quark loops to the evolution kernel introduces terms which explicitly break the scaling property (4), similar to what was found for the Reggeon [8] (see also [24]). Therefore, we set aside the question of generalizing this approach to the large- N_c & N_f limit as a separate project, which we leave for future work.

Acknowledgments

The authors are greatly indebted to Edmond Iancu for his suggestion to look for a scaling solution to the helicity evolution equations and to Bin Wu for several helpful discussions of the involved integrals.

This material is based upon work supported by the U.S. Department of Energy, Office of Science, Office of Nuclear Physics under Award Number DE-SC0004286 (YK), within the framework of the TMD Topical Collaboration (DP), and DOE Contract No. DE-AC52-06NA25396 (MS). MS received additional support from the U.S. Department of Energy, Office of Science under the DOE Early Career Program.

References

- [1] E. A. Kuraev, L. N. Lipatov, V. S. Fadin, The Pomeron singularity in non-Abelian gauge theories, *Sov. Phys. JETP* 45 (1977) 199–204.
- [2] I. Balitsky, L. Lipatov, The Pomeron Singularity in Quantum Chromodynamics, *Sov. J. Nucl. Phys.* 28 (1978) 822–829.
- [3] R. Kirschner, L. Lipatov, Double Logarithmic Asymptotics and Regge Singularities of Quark Amplitudes with Flavor Exchange, *Nucl. Phys.* B213 (1983) 122–148. doi:10.1016/0550-3213(83)90178-5.
- [4] R. Kirschner, Regge Asymptotics of Scattering Amplitudes in the Logarithmic Approximation of QCD, *Z. Phys.* C31 (1986) 135. doi:10.1007/BF01559604.
- [5] R. Kirschner, Regge asymptotics of scattering with flavor exchange in QCD, *Z. Phys.* C67 (1995) 459–466. arXiv:hep-th/9404158, doi:10.1007/BF01624588.
- [6] R. Kirschner, Reggeon interactions in perturbative QCD, *Z. Phys.* C65 (1995) 505–510. arXiv:hep-th/9407085, doi:10.1007/BF01556138.
- [7] S. Griffiths, D. Ross, Studying the perturbative Reggeon, *Eur. Phys. J.* C12 (2000) 277–286. arXiv:hep-ph/9906550, doi:10.1007/s100529900240.
- [8] K. Itakura, Y. V. Kovchegov, L. McLerran, D. Teaney, Baryon stopping and valence quark distribution at small x , *Nucl. Phys.* A730 (2004) 160–190. arXiv:hep-ph/0305332, doi:10.1016/j.nuclphysa.2003.10.016.
- [9] J. Bartels, B. Ermolaev, M. Ryskin, Nonsinglet contributions to the structure function g_1 at small x , *Z. Phys.* C70 (1996) 273–280. arXiv:hep-ph/9507271.
- [10] J. Bartels, B. I. Ermolaev, M. G. Ryskin, Flavor singlet contribution to the structure function $G(1)$ at small x , *Z. Phys.* C72 (1996) 627–635. arXiv:hep-ph/9603204, doi:10.1007/BF02909194, 10.1007/s002880050285.
- [11] Y. V. Kovchegov, D. Pitonyak, M. D. Sievert, Helicity Evolution at Small x , *JHEP* 01 (2016) 072. arXiv:1511.06737, doi:10.1007/JHEP01(2016)072.
- [12] Y. V. Kovchegov, D. Pitonyak, M. D. Sievert, Helicity Evolution at Small x : Flavor Singlet and Non-Singlet Observables, *Phys. Rev. D* 95 (1) (2017) 014033. arXiv:1610.06197, doi:10.1103/PhysRevD.95.014033.
- [13] I. Balitsky, Operator expansion for high-energy scattering, *Nucl. Phys.* B463 (1996) 99–160. arXiv:hep-ph/9509348, doi:10.1016/0550-3213(95)00638-9.
- [14] I. Balitsky, Factorization and high-energy effective action, *Phys. Rev. D* 60 (1999) 014020. arXiv:hep-ph/9812311.
- [15] I. Balitsky, Operator expansion for high-energy scattering, *Nucl. Phys.* B463 (1996) 99–160. arXiv:hep-ph/9509348.
- [16] Y. V. Kovchegov, Small- x F_2 structure function of a nucleus including multiple pomeron exchanges, *Phys. Rev. D* 60 (1999) 034008. arXiv:hep-ph/9901281.
- [17] Y. V. Kovchegov, Unitarization of the BFKL pomeron on a nucleus, *Phys. Rev. D* 61 (2000) 074018. arXiv:hep-ph/9905214.
- [18] J. Jalilian-Marian, A. Kovner, H. Weigert, The Wilson renormalization group for low x physics: Gluon evolution at finite parton density, *Phys. Rev. D* 59 (1998) 014015. arXiv:hep-ph/9709432.
- [19] J. Jalilian-Marian, A. Kovner, A. Leonidov, H. Weigert, The Wilson renormalization group for low x physics: Towards the high density regime, *Phys. Rev. D* 59 (1998) 014014. arXiv:hep-ph/9706377.
- [20] E. Iancu, A. Leonidov, L. D. McLerran, The renormalization group equation for the color glass condensate, *Phys. Lett.* B510 (2001) 133–144. doi:10.1016/S0370-2693(01)00524-X.
- [21] E. Iancu, A. Leonidov, L. D. McLerran, Nonlinear gluon evolution in the color glass condensate. I, *Nucl. Phys.* A692 (2001) 583–645. arXiv:hep-ph/0011241.
- [22] Y. V. Kovchegov, D. Pitonyak, M. D. Sievert, Small- x asymptotics of the quark helicity distribution, *Phys. Rev. Lett.* 118 (5) (2017) 052001. arXiv:1610.06188, doi:10.1103/PhysRevLett.118.052001.
- [23] E. R. Nocera, E. Santopinto, Can sea quark asymmetry shed light on the orbital angular momentum of the proton? arXiv:1611.07980.
- [24] E. Iancu, J. D. Madrigal, A. H. Mueller, G. Soyez, D. N. Triantafyllopoulos, Resumming double logarithms in the QCD evolution of color dipoles, *Phys. Lett.* B744 (2015) 293–302. arXiv:1502.05642, doi:10.1016/j.physletb.2015.03.068.